Bioelectrochemistry 74 (2008) 217–221

Contents lists available at ScienceDirect

Bioelectrochemistry

journal homepage: www.elsevier.com/locate/bioelechem

# Facile electrocatalytic redox of hemoglobin by flower-like gold nanoparticles on boron-doped diamond surface

Mingfang Li, Guohua Zhao *, Rong Geng, Huikang Hu

*Department of Chemistry, Tongji University, Shanghai, 200092, China*

ARTICLE INFO

*Article history:*
Received 24 October 2007
Received in revised form 11 August 2008
Accepted 11 August 2008
Available online 19 August 2008

*Keywords:*
Flower-like gold nanoparticles
Electrochemical property
Electron transfer-bridge
Different electrocatalytical activity

ABSTRACT

The flower-like gold nanoparticles together with spherical and convex polyhedron gold nanoparticles were fabricated on boron-doped diamond (BDD) surface by one-step and simple electrochemical method through easily controlling the applied potential and the concentration of $HAuCl_4$. The recorded X-ray diffraction (XRD) patterns confirmed that these three shapes of gold nanoparticles were dominated by different crystal facets. The cyclic voltammetric results indicated that the morphology of gold nanoparticles plays big role in their electrochemical behaviors. The direct electrochemistry of hemoglobin (Hb) was realized on all the three different shapes of nanogold-attached BDD surface without the aid of any electron mediator. In pH 4.5 acetate buffer solutions (ABS), Hb showed a pair of well defined and quasi-reversible redox peaks. However, the results obtained demonstrated that the redox peak potential, the average surface concentration of electroactive heme, and the electron transfer rates of Hb are greatly dependent upon the surface morphology of gold nanoparticles. The electron transfer rate constant of hemoglobin over flower-like nanogold/BDD electrode was more than two times higher than that over spherical and convex polyhedron nanogold. The observed differences may be ascribed to the difference in gold particle characteristics including surface roughness, exposed surface area, and crystal structure.



## 1. Introduction

As a high performance material with many extreme properties, conductive boron-doped diamond (BDD) is an alternative to traditional carbon electrodes that provides superior chemical and physical features including a wide electrochemical potential window in either aqueous or non-aqueous media, very low capacitance, low background currents, low adsorption of organic molecules, high electrochemical stability, and high resistance to fouling and insensitivity to dissolved oxygen [1–3]. The properties mentioned above make BDD an ideal substrate for biosensor. However, it is usually very difficult for redox protein to realize direct electron transfer on as-grown BDD electrode. Many methods have been developed to modify or immobilize different biocompatible materials on BDD surface to promote the electron transfer [4–7].

Metal nanoparticles are attracting increasing attention in recent time and have been used in many electrochemical, electroanalytical and bioelectrochemical applications owing to their interesting size and large specific surface area and extraordinary electrocatalytic activity which are entirely different from their bulk metal counterparts [8–12]. Gold nanoparticles, in particular, have been widely used to bioanalytical applications and the construction of biosensor because of their excellent ability to immobilize biomolecules and at the same time retain the biocatalytic activities of those biomolecules [13–16].

Hemoglobin (Hb) is a kind of heme protein that contains four polypeptide chains, each of which has one electroactive iron heme as a prosthetic group. Hb stores in blood and functions as oxygen deliverer which is of great help to living activities. Investigation of the heterogeneous electron transfer process between electrode surface and Hb is very important for the fundamental studies as well as the impetus for the further developments of bioreactors and biosensors. However, Hb displays poor redox kinetics at conventional electrodes due to the sluggish electron transfer. As we know, the electroactive center of Hb is usually buried deeply inside the non-conductive peptide chains, resulting in inaccessibility of its electroactive center to the electrode surface. On the other hand, this slow electron transfer may be caused by the unfavorable orientation of Hb molecules on the electrode surface, which increases the distance between its heme center and electrode surface, and the adsorption of impurities, which block the electron communication between heme and electrode and make it denature. Thus, the investigation of the direct electrochemistry of Hb is of importance for the understanding of the structure-function relationship of Hb. Many researchers have focused their attentions on the enhancement of the electron transfer of Hb by using nanostructured gold as mediators or promoters [17–22]. Gold nanoparticles have been attached onto glassy carbon electrode surface through sulfhydryl-terminated monolayer and a pair of well-defined

* Corresponding author. Tel.: +86 21 65981180; fax: +86 21 65982287.
*E-mail addresses:* g.zhao@mail.tongji.edu.cn, ghzhao.tongji@hotmail.com, ghzhao@tongji.edu.cn (G. Zhao).

1567-5394/$ – see front matter © 2008 Elsevier B.V. All rights reserved.
doi:10.1016/j.bioelechem.2008.08.004

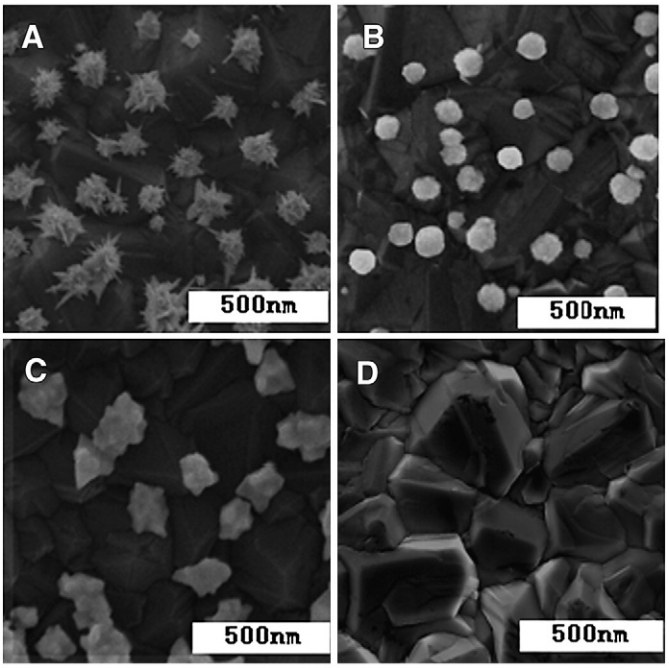


**Fig. 1.** SEM images of the gold nanoparticles electrodeposited on BDD surface (A) Flower-like nanogold prepared from 0.2 M $H_2SO_4$ solution containing 2 mM $HAuCl_4$ and (B) Spherical nanogold prepared from 0.2 M $H_2SO_4$ solution containing 0.2 mM $HAuCl_4$ with the deposition potential at +0.5 V vs Ag/AgCl, (C) Convex polyhedron nanogold prepared from 0.2 M $H_2SO_4$ solution containing 2 mM $HAuCl_4$ with the deposition potential at −0.1 V vs Ag/AgCl, (D) bare BDD.

redox peaks with formal potential of about −0.085 V for Hb was obtained on this modified glass carbon electrode. The apparent heterogeneous electron transfer rate constant was 1.05 $s^{-1}$ [19]. The direct electrochemical behavior of Hb on gold nanoshells modified indium tin oxide electrode has been investigated and the formal potential obtained on this modified electrode was −0.265 V, and the electron transfer rate constant was 2.39 $s^{-1}$ [21]. Hb was immobilized successfully on nanometer-sized gold colloid particles associated with a cysteamine monolayer on a gold electrode surface, and the direct electron transfer between Hb and the modified electrode was achieved; the formal potential of Hb was −0.051 V and the electron transfer rate constant was 0.49 $s^{-1}$ [22]. As we can see, the size, shape of the metal nanoparticles and the substrate on which nanostructured gold modified play key role in the electrochemical behavior of Hb. Therefore, in this work, different morphology of gold nanoparticles will be electrodeposited on BDD substrate and their electrocatalytical activities to Hb will be investigated.

In our present researches, a simple way was introduced to prepare the size, shape and crystallinity controlled gold nanoparticles, and the flower-like, spherical, and convex polyhedron gold nanoparticles with different dominant crystal facets have been easily fabricated by one step and low cost electrochemical method under various conditions. The different electrochemical behaviors of these three different shapes of gold nanoparticles were compared. The three different gold nanoparticles functioned as an electron transfer-bridge between BDD and Hb was studied, and the different electrocatalytic behavior of three different shapes of gold nanoparticles to Hb was obtained. The effects of surface roughness, exposed surface area, and crystal structure of gold nanoparticles on electrocatalytic activity to Hb were investigated.

## 2. Experimental

Chloroauric acid and hemoglobin were purchased from sigma chemicals and used as received. Sulfuric acid, ferrous potassium cyanide and other chemicals from Shanghai Reagent Co., Ltd were of analytical grade and used without further purification. Buffers were acetate buffer solutions (ABS). Twice deionized water was used for preparing electrolyte solutions. And the boron-doped diamond grew with a microwave plasma chemical vapor deposition was obtained from CSEM, Swiss.

The BDD was first anodized at +2.8 V in 1 M $H_2SO_4$ for 10 s to remove any impurities on its surface. The gold nanoparticles was electrochemically deposited on BDD by potentiostatic method from an aqueous solution containing 2 mM, 0.2 mM $HAuCl_4$ and 0.2 M $H_2SO_4$ after the BDD was pretreated by scanning the potential from −2.8 V to 0 V and then back to −2.8 V for 10 cycles at a sweep rate of 50 mV/s, and the resulting Au/BDD was dipped into 0.2 M ABS containing 50 μM hemoglobin (Hb) for 72 h to obtain Hb/Au/BDD modified electrode.

All electrochemical experiments were carried out on a CHI 660C electrochemical workstation (CH Instrument CO., USA). Traditional three-electrode system involving a platinum wire as counter-electrode and a KCl-saturated Ag/AgCl electrode as a reference electrode was employed for electrodeposition and electrochemical characterization. Voltammetric experiments at modified electrodes were performed in buffers containing no proteins. Buffers were purged with highly purified nitrogen for at least 10 min prior to a series of experiments. A nitrogen atmosphere was then maintained during the whole experiment.

The scanning electron microscope (SEM) image was obtained using Quanta 200 FEG (FEI Company, Japan). The XRD pattern was obtained

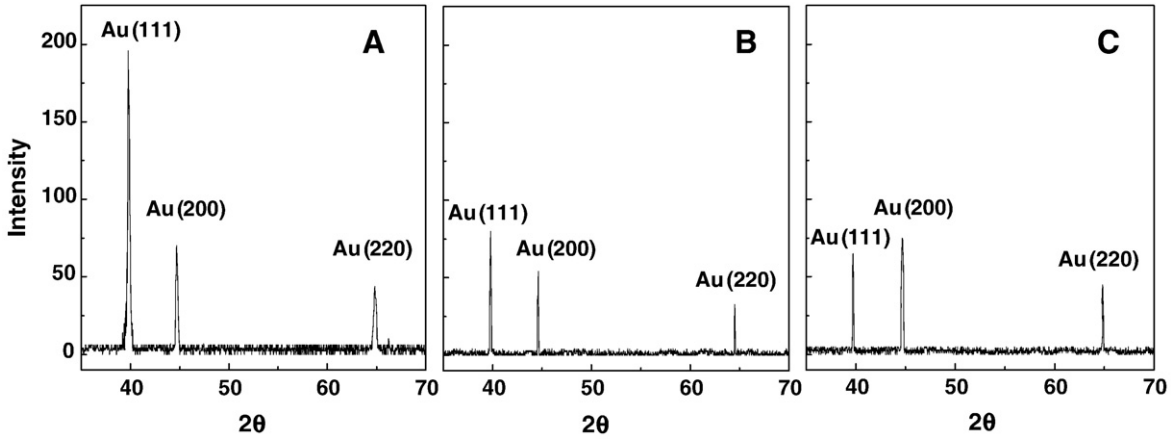


**Fig. 2.** XRD patterns of (A) Flower-like gold nanoparticles (B) Spherical gold nanoparticles (C) Convex polyhedron gold nanoparticles.

**Table 1**
The parameters obtained on different morphology of gold nanoparticles modified BDD

| | Flower-like | Spherical | Convex polyhedron |
|---|---|---|---|
| Diameter of nanogold/nm | 100–150 | 70–100 | 100–150 |
| $I_{Au(111)}/I_{Au(200)}$ | 2.82 | 1.43 | 0.87 |
| $R_{ct}$ /Ω (After adsorption of Hb) | 6000 | 4100 | 2900 |
| $\Gamma^*/10^{-10}$ mol cm$^{-2}$ | 2.95 | 2.59 | 1.99 |
| $k_s/s^{-1}$ | 0.34 | 0.16 | 0.13 |

by a D/max2550VB3+/PC X-ray diffractometer using Cu (40 kV, 100 mA).

All the results in this paper represent the average over three parallel experiments.

## 3. Results and discussion

### 3.1. Morphology and XRD patterns of gold nanoparticles on BDD

Gold nanoparticles were prepared by one-step potentiostatic method under various experimental conditions and its surface morphology was characterized by SEM (shown in Fig. 1A, B, and C respectively). For comparison, the typical SEM image of as-grown BDD film was shown in Fig. 1D, a columnar, randomly textured, polycrystalline film and grains of an average size of 300–500 nm are clearly observed. As shown in Fig. 1A, deposition from 2 mM HAuCl4 solutions at the applied potential of +0.5 V gave the beautiful flower-like nanostructure of gold particles. From the SEM image, we can see that the particle size of the flower-like nanogold is ranging from 100 nm to 150 nm; the gold nanoparticles look very pretty, just like many flowers blossom on BDD surface, and the keen-edged leaves make the surface of nanostructured gold particles very rough and numerous flower leaves possess large exposed surface area. When a lower concentration of $HAuCl_4$ (0.2 mM) was used, a regular but featureless spherical nanostructured-gold with the particle size of 70–100 nm was obtained. We can see that the spherical gold nanoparticles with large specific surface area were evenly distributed on BDD surface. To investigate the effects of deposition potential on the formation of gold particle, a comparative study was performed. A more negative potential, −0.1 V, was applied to BDD electrode, another shape of convex polyhedron nanoparticles with very irregular face (Fig. 1C) which is far from flower and sphere can be obtained from 2 mM $HAuCl_4$ solution. The grain size of this convex polyhedron is ranging from 150 to 200 nm. As it can be seen, the convex polyhedron gold nanoparticles cling tightly onto BDD surface; therefore, the exposed surface area is relatively small.

The crystalline nature of the gold nanoparticles was confirmed by the corresponding XRD patterns. The XRD diffraction peaks of the electrodeposited flower-like, spherical, and convex polyhedron gold particles are shown in Fig. 2 (A–C). The observed three sharp peaks in Fig. 2 can be assigned to the (111), (200) and (220) facets of metal gold, respectively, indicating that the nanoparticles are composed of pure crystalline gold with the face-centered cubic structure. Fig. 2A shows that the intensity of Au (111) peak obtained for the flower-like particles is much higher than that of Au (200) and Au (220) peaks, indicating that the flower-like gold nanoparticles is preferentially dominated by Au (111) facet. From Fig. 2B and C, we can see that the intensity of Au (111) peak for spherical gold particles is only a slightly higher than that of Au (200) peaks, but for convex polyhedron gold particles, the intensity of Au (111) peak is lower than that of Au (200) peaks. The intensity ratio of Au (111) peak to Au (200) peak for three kinds of gold nanoparticles is shown in Table 1.

### 3.2. Electrochemical characterization of different morphology of nanogold

Fig. 3 depicts the cyclic voltammograms (CVs) obtained on different gold nanoparticles modified BDD electrodes in 0.1 M $H_2SO_4$. An interesting thing can be seen from Fig. 3A and B. Compared with CV curve obtained on bare BDD (Fig. 3D), two obvious oxidation peaks at about +1.4 V and +1.1 V can be observed on both flower-like and spherical gold nanoparticles modified BDD electrode. However, on flower-like gold nanoparticles modified BDD electrode, the peak current at +1.4 V is much higher than that at +1.1 V, while the peak currents of these two peaks equal to each other on spherical gold nanoparticles modified BDD electrode. Meanwhile, we can see that the oxidation peak current at about +1.4 V on flower-like gold nanoparticles modified BDD electrode is evidently larger than that on spherical gold. From Fig. 3C, we can see only one oxidation peak at +1.1 V can be observed on convex polyhedron gold nanoparticles modified BDD electrode and the oxidation peak near +1.4 V is very unconspicuous and ill-defined. From the data mentioned above, it can be deduced that the oxidation peak at +1.4 V is characteristic of the Au (111) surface and the oxidation peak at +1.1 V is characteristic of the Au (200) or Au (220) surface. The result agrees with the XRD pattern very well.

### 3.3. Electrocatalysis of different morphology of nanogold to Hb

Alternative current (AC) impedance spectroscopy on BDD electrode after the modification of different morphologies of gold nanoparticles and the adsorption of Hb was further measured in the presence of equimolar $[Fe(CN)6]^{3-/4-}$, as shown in Fig. 4. Fig. 4D shows the impedance spectrum of the bare BDD electrode. We can see that the charge transfer resistance ($R_{ct}$) of $[Fe(CN)6]^{3-/4-}$ obtained on bare BDD is very large and the calculated Rct for the $[Fe(CN)6]^{3-/4-}$ redox

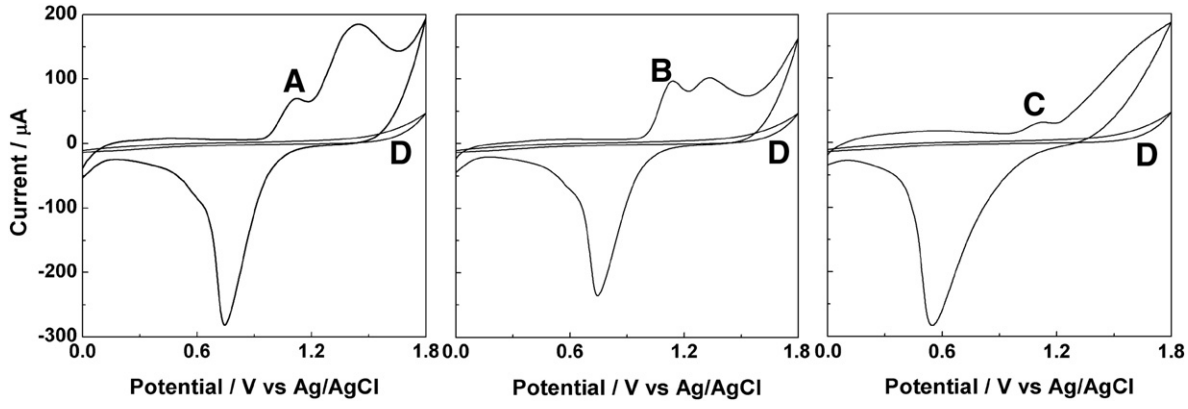


**Fig. 3.** Cvs of (A) flower-like gold nanoparticles (B) spherical gold nanoparticles (C) convex polyhedron gold nanoparticles modified BDD electrode (D) bare BDD in 0.1 M $H_2SO_4$.

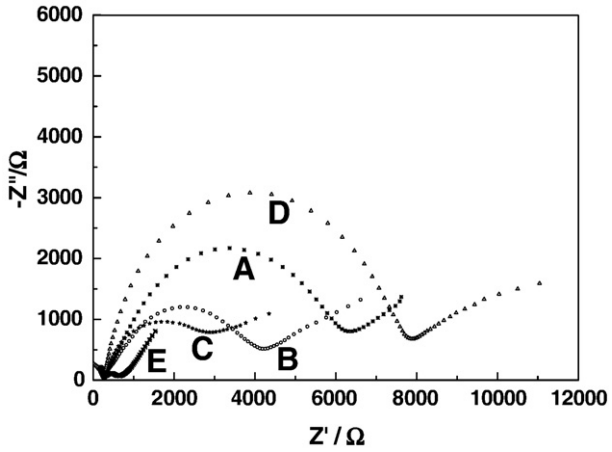


**Fig. 4.** Electrochemical impedance spectroscopy of (A) Hb/flower-like nanogold/BDD (B) Hb/spherical gold/BDD (C) Hb/convex polyhedron gold/BDD (D) Bare BDD (E) Flower-like gold/BDD electrode in 5 mM $K_3Fe(CN)_6/K_4Fe(CN)_6$ (1:1) containing 0.10 M KCl. Applied potential: 0.20 V; frequency range: 0.1 Hz to 100 kHz.

couple was 7800 Ω. $R_{ct}$ was decreased to 260 Ω when gold nanoparticles were modified onto BDD electrode surface and then greatly increased to higher than 2500 Ω after the incubation of Hb on Au/BDD electrode. An interesting thing can be observed from Fig. 4: the Rct value of $[Fe(CN)6]^{3-/4-}$ obtained on flower-like gold/BDD almost equals that obtained on spherical and convex polyhedron gold/BDD owing to the excellent electrical conductivity of gold. However, when Hb was trapped on Au/BDD surface, the Rct values differ greatly from each other, as was shown in Table 1. We can see that the charge transfer resistance increased in the following order: Hb/flower-like nanogold /BDD>Hb/spherical nanogold /BDD>Hb/convex polyhedron nanogold /BDD. This order is consistent with the order of exposed surface area for three different shapes of gold nanoparticles.

CVs of different electrodes were measured in 0.2 M ABS (pH 4.5) at a sweep rate of 100 mV/s, as shown in Fig. 5. Compared with Au/BDD electrode, the Hb/Au/BDD electrode gave a couple of well-defined redox peaks with formal potential of +0.251 V, +0.261 V, +0.283 V for Hb/flower-like nanogold /BDD, Hb/spherical nanogold/BDD and Hb/convex polyhedron nanogold/BDD electrodes, respectively, confirming that the redox peaks on Hb/nanoAu/BDD electrode were attributed to the electroactive heme center in Hb molecules. But a difference still can be seen. At Hb/flower-like gold/BDD electrode, the oxidation peak for heme center is at +0.339 V with the reduction peak potential near +0.164 V, and the peak-to-peak separation ($\Delta E$p) is 0.175 V. while at Hb/spherical gold/BDD and Hb/convex polyhedron gold/BDD electrodes, the oxidation peak is positively shifted and the reduction peak

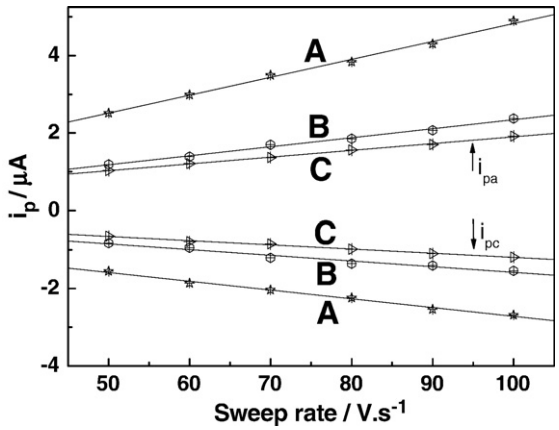


**Fig. 6.** Plot of the cathodic and anodic peak currents vs. sweep rate (A) Hb/flower-like gold/BDD (B) Hb/spherical gold/BDD (C) Hb/convex polyhedron gold/BDD electrodes in pH 4.5 ABS.

shifted negatively, and $\Delta E$p was widened to 0.262 V and 0.290 V respectively.

More measurements were made to further understand the direct electrochemistry of hemoglobin on these three different electrodes. Fig. 5 shows the CVs obtained on Hb/flower-like/BDD, Hb/spherical gold/BDD, and Hb/convex polyhedron gold/BDD electrodes in ABS solutions at different sweep rates. It is can be seen, both the peak currents and the peak potential separation ($\Delta E$p) between the cathodic and anodic peaks increase as the scan rate increases. The linear relationship between the cathodic peak current and scan rate in the range of 0.05–0.1 V/s (Fig. 6) indicates that the electron transfer between Hb and three gold nanoparticles modified BDD electrodes is a surface-controlled quasi-reversible process.

For Hb on flower-like/BDD electrode, the peak-to-peak separations of the cyclic voltammograms at 50, 60, 70, 80, 90 and 100 mV/s were 138, 145, 152, 159, 169, and 175 mV, respectively (see Fig. 5A). Supposing the charge transfer coefficient was between 0.3 and 0.7, the electron transfer rate constant ($k_s$) was estimated to be 0.34 $s^{-1}$ according to Laviron's model with the formula

$$k_s = mnF\upsilon/RT \quad (1)$$

where $m$ is a parameter related to the peak-to-peak separation [23].

The anodic and cathodic peak potentials are linearly dependent on the logarithm of scan rates ($\upsilon$) when $\Delta E$p>200/$n$ (Fig. 5B and C), which is in agreement with the Laviron theory [23]: a plot of $E$p versus log $\nu$ yields two straight lines with slopes, for the cathodic peak, the slope is $-2.3RT/\alpha nF$ and for the anodic peak, the slope is $2.3RT/(1-\alpha)nF$. The electron transfer rate constant ($k_s$) can be estimated to be 0.16

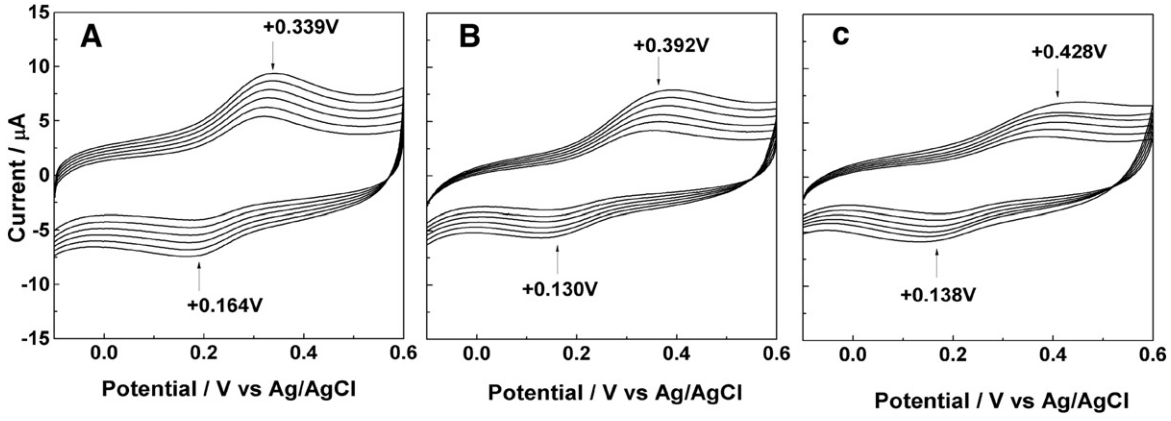


**Fig. 5.** Cvs of (A) Hb/flower-like nanogold/BDD (B) Hb/spherical nanogold/BDD (C)Hb/convex polyhedron nanogold/BDD electrodes in pH 4.5 ABS at the sweep rates of 0.05, 0.06, 0.07, 0.08, 0.09, 0.1 V/s (from inner to outer).

and 0.13 $s^{-1}$ for Hb on spherical and convex polyhedron gold nanoparticles modified BDD electrode, respectively, according to the following equation developed by Laviron.

$$\lg k_s = \alpha\lg(1-\alpha) + (1-\alpha)\lg\alpha - \lg(RT/nF\upsilon) - \alpha(1-\alpha)nF\Delta E_p/2.3RT \quad (2)$$

With the results forementioned, it can be concluded that the electron transfer rate constant of electrode reaction increases in the following order: Hb/flower-like nanogold/BDD>Hb/spherical nanogold/BDD>Hb/convex polyhedron nanogold/BDD, indicating that the electrocatalysis of flower-like nanogold to Hb is the strongest, then the spherical nanogold, and that of convex polyhedron nanogold is the weakest.

To further understand the different electrocatalysis of different morphology of nanogold to Hb, the average surface concentration of electroactive species was calculated. According to $Q=nFA\Gamma^*$ [24], the amount of electroactive species adsorbed on electrode surface can be easily obtained by integration of CV peaks. Here $Q$ is the charge, $n$ is the number of electrons transferred, $F$ is Faraday's constant and $A$ is the working electrode area. From the data in Fig. 5, the surface concentration ($\Gamma^*$) of Hb on the flower-like gold/BDD, spherical gold/BDD, and convex polyhedron gold/BDD were estimated to be 2.95, 2.59, and $1.99\times10^{-10}$ mol $cm^{-2}$, respectively.

As is known to us, the chemical properties of the nano-structured metal are tuned with its size, shape, and crystallinity, and then the electrocatalytical activity of metal particles is evidently determined by their physical and chemical properties. Firstly, we can assume that the topography of gold nanoparticles plays a very significant role and has a substantial impact on the adsorption and electrochemistry of Hb. As shown in Fig. 1, the flower-like gold nanoparticles displays the roughest surface and the largest exposed surface area and exhibits a surface texture that appears more optimal for Hb adsorption and electrochemical response, so we can obtain the fastest direct electron transfer process between Hb and flower-like gold/BDD. The topography of convex polyhedron gold nanoparticles is relatively smoothest and flattest with the smallest exposed surface area; the morphology of this style is poor for the adsorption and electrochemistry of biomacromolecules. Then the slowest electron transfer rate constant of electrode reaction is obtained on Hb/convex polyhedron gold/BDD. The crystallinity of the resulting gold nanoparticles plays another crucial role in its electrocatalysis to Hb. From the XRD results and electrochemical characterization in 0.1 M $H_2SO_4$, we know that the intensity of the Au (111) peak for the flower-like particles is much higher than that for spherical and convex polyhedron gold particles. The experimental results indicate that the more highly the surface is dominated by Au (111), the faster the electron transfer rate of Hb is observed. We can presume that the Au (111) of gold nanoparticle is more active to redox of Hb than that of Au (200) and Au(220) facets.

## 4. Conclusions

The flower-like, spherical, and convex polyhedron gold nanoparticles were fabricated on BDD surface by easily manipulating the electrodeposition potential and the concentration of $HAuCl_4$. Experimental results show that the electrochemical properties of these gold nanoparticles with different morphologies are quite distinct from each other. The gold nanoparticles attached on BDD electrode can function as an electron transfer bridge between Hb and BDD surface. The redox of hemoglobin immobilized on three different structures of gold particles shows a surface controlled process with the apparent heterogeneous electron transfer rate constant of 0.34 $s^{-1}$, 0.16 $s^{-1}$, and 0.13 $s^{-1}$, respectively.

## Acknowledgement

The authors are deeply grateful for the support of the National Natural Science Foundation of China (No. 20577035) and Nanometer Science Foundation of Shanghai, China (No. 0652nm030).

## References

[1] H.R. Gu, X.D. Su, K.P. Loh, Electrochemical impedance sensing of DNA hybridization on conducting polymer film-modified diamond, J. Phys. Chem., B 109 (2005) 13611–13618.
[2] K.L. Soh, W.P. Kang, J.L. Davidson, Y.M. Wong, A. Wisitsora-at, G. Swain, D.E. Cliffel, CVD diamond anisotropic film as electrode for electrochemical sensing, Sens. Actuators, B 91 (2003) 39–45.
[3] T.N. Rao, I. Yagi, T. Miwa, D.A. Tryk, A. Fujishima, Electrochemical oxidation of NADH at highly boron-doped diamond electrodes, Anal. Chem. 71 (1999) 2506–2511.
[4] I. Yagi, T. Ishida, K. Uosaki, Electrocatalytic reduction of oxygen to water at Au nanoclusters vacuum-evaporated on boron-doped diamond in acidic solution, Electrochem. Commun. 6 (2004) 773–779.
[5] Y. Coffinier, S. Szunerits, C. Jama, R. Desmet, O. Melnyk, B. Marcus, L. Gengembre, E. Payen, D. Delabouglise, R. Boukherroub, Peptide immobilization on amine-terminated boron-doped diamond surfaces, Langmuir 23 (2007) 4494–4497.
[6] Y.L. Zhou, R.H. Tian, J.F. Zhi, Amperometric biosensor based on tyrosinase immobilized on a boron-doped diamond electrode, Biosens. Bioelectron. 22 (2007) 822–828.
[7] H. Uetsuka, D.C. Shin, N. Tokuda, K. Saeki, C.E. Nebel, Electrochemical grafting of boron-doped single-crystalline chemical vapor deposition diamond with nitrophenyl molecules, Langmuir 23 (2007) 3466–3472.
[8] D. Renedo, M.J.A. Martínez, A novel method for the anodic stripping voltammetry determination of Sb(III) using silver nanoparticle-modified screen-printed electrodes, Electrochem. Commun. 9 (2007) 820–826.
[9] M. Chikae, K. Idegami, K. Kerman, N. Nagatani, M. Ishikawa, Y. Takamura, E. Tamiya, Direct fabrication of catalytic metal nanoparticles onto the surface of a screen-printed carbon electrode, Electrochem. Commun. 8 (2006) 1375–1380.
[10] T. You, O. Niwa, M. Tomita, S. Hirono, Characterization of platinum nanoparticle-embedded carbon film electrode and its detection of hydrogen peroxide, Anal. Chem. 75 (2003) 2080–2085.
[11] T.Y. You, O. Niwa, Z.L. Chen, K. Hayashi, M. Tomita, S. Hirono, An amperometric detector formed of highly dispersed Ni nanoparticles embedded in a graphite-like carbon film electrode for sugar determination, Anal. Chem. 75 (2003) 5191–5196.
[12] J.M. Zen, C.T. Hsu, A.S. Kumar, H.J. Lyuu, K.Y. Lin, Amino acid analysis using disposable copper nanoparticle plated electrodes, Analyst 129 (2004) 841–845.
[13] V. Carralero, M.L. Mena, A. Gonzalez-Cortés, P. Yáñez-Sedeño, J.M. Pingarrón, Development of a high analytical performance-tyrosinase biosensor based on a composite graphite – teflon electrode modified with gold nanoparticles, Biosens. Bioelectron. 22 (2006) 730–736.
[14] M.T. Castañeda, A. Merkoci, M. Pumera, S. Alegret, Electrochemical genosensors for biomedical applications based on gold nanoparticles, Biosens. Bioelectron. 22 (2007) 1961–1967.
[15] L. Wang, J.Y. Bai, P.F. Huang, H.J. Wang, L.Y. Zhang, Y.Q. Zhao, Self-assembly of gold nanoparticles for the voltammetric sensing of epinephrine, Electrochem. Commun. 8 (2006) 1035–1040.
[16] X.L. Li, J. Wu, N. Gao, G.L. Shen, R.Q. Yu, Electrochemical performance of l-cysteine–gold particle nanocomposite electrode interface as applied to preparation of mediator-free enzymatic biosensors, Sens. Actuators, B 117 (2006) 35–42.
[17] M.X. Li, M.T. Xu, N.Q. Li, Z.N. Gu, X.H. Zhou, Electrocatalysis of hemoglobin at $C_{70}$/DDAB films in an aqueous solution, J. Phys. Chem., B 106 (2002) 4197–4202.
[18] W. Sun, R.F. Gao, K. Jiao, Electrochemistry and electrocatalysis of hemoglobin in Nafion/nano-$CaCO_3$ film on a new ionic liquid $BPPF_6$ modified carbon paste electrode, J. Phys. Chem., B 111 (2007) 4560–4567.
[19] L. Zhang, X.E. Jiang, E.K. Wang, S.J. Dong, Attachment of gold nanoparticles to glassy carbon electrode and its application for the direct electrochemistry and electrocatalytic behavior of hemoglobin, Biosens. Bioelectron. 21 (2005) 337–345.
[20] L.W. Du, H. Jiang, X.H. Liu, E.K. Wang, Biosynthesis of gold nanoparticles assisted by *Escherichia coli* DH5α and its application on direct electrochemistry of hemoglobin, Electrochem. Commun. 9 (2007) 1165–1170.
[21] Y. Wang, W.P. Qian, Y. Tan, S.H. Ding, H.Q. Zhang, Direct electrochemistry and electroanalysis of hemoglobin adsorbed in self-assembled films of gold nanoshells, Talanta 72 (2007) 1134–1140.
[22] H.Y. Gu, A.M. Yu, H.Y. Chen, Direct electron transfer and characterization of hemoglobin immobilized on a Au colloid-cysteamine-modified gold electrode, J. Electroanal. Chem. 516 (2001) 119–126.
[23] E. Laviron, General expression of the linear potential sweep voltammogram in the case of diffusionless electrochemical systems, J. Electroanal. Chem. 101 (1979) 19–28.
[24] C.X. Cai, J. Chen, Direct electron transfer and bioelectrocatalysis of hemoglobin at a carbon nanotube electrode, Anal. Biochem. 325 (2004) 285–292.